Morphological, structural, thermal and degradation properties of polylactic acid-waxy maize starch nanocrystals based nanocomposites prepared by melt processing

Pooja Takkalkar, Mahalaxmi Ganapathi, Maha Al-Ali, Nhol Kao*, Gregory Griffin

Chemical and Environmental Engineering, School of Engineering, RMIT University, Melbourne, 3000, Australia

*****Corresponding author: Tel: (+61) 39925 3257; Fax: (+61) 39639 0138; E-mail: nhol.kao@rmit.edu.au

DOI: 10.5185/amlett.2019.2185
www.vbripress.com/aml

Abstract

Currently used petroleum-based polymers have adversely affected the environment in various ways, mainly due to their non-biodegradability. This undesirable aspect of commercial polymers led to increased interest in the research area of biodegradable polymer nanocomposites. Polylactic acid (PLA) based nanocomposites, with three different loadings of waxy maize starch nanocrystals (WSNC) as nanofiller (1, 3 and 5 wt%), were melt-blended in a Haake Rheomix. The morphological, structural, thermal and abiotic degradation characteristics of the prepared PLA-WSNC nanocomposites were studied to determine the effects of adding WSNC at different loadings in PLA. The results indicated that WSNC were dispersed uniformly at lower loadings (0-3 wt%) and agglomerated at higher loadings (5 wt%) within the PLA matrix. All PLA-WSNC nanocomposites were found to be stable over the processing temperature range of 25-220 ºC. In addition, there was no considerable change in the glass transition temperature and the melting point of the nanocomposites. Though, the cold crystallization temperature was reduced with the increase of WSNC loadings. The abiotic degradation studies, used as an initial screening tool, indicated that WSNC can accelerate the degradation process of PLA. As a result, the degradation rate was improved for all the PLA-WSNC nanocomposites. The PLA-WSNC-3 wt% was found to be the optimum concentration to enhance the crystallinity and morphological property of PLA, and beyond that the properties were affected by agglomeration.

Keywords: Polylactic acid, waxy maize starch nanocrystals, melt processing.

Statement of Novelty

The objective of this research was to examine the influence of WSNC concentration on the morphological, thermal, structural properties and to develop a quick and easy standard method to determine the extent of degradation of PLA-WSNC nanocomposites. The PLA-WSNC nanocomposites were prepared by melt processing in a Haake rheomix to be used as an environmentally friendly packaging film. The thermal and morphological study indicated that the optimum concentration of WSNC to improve the properties of PLA was 3 wt%, beyond which the WSNC started to agglomerate. WSNC accelerated the extent of degradation of PLA when the nanofiller concentration increased from 1 wt% to 5 wt%. The abiotic method proved effective as safe, easy and quick laboratory scale screening tool for determining biodegradability of PLA based nanocomposites.

Introduction

The demand for the generation of environment friendly material is rising, due to the problems posed by extensive use of petroleum-based products. One of the "green" materials emerging in the market nowadays is biodegradable polymer nanocomposites. Nanocomposites consist of a bio-based polymer matrix incorporated with nanofiller having at least one dimension in 1–100 nm range [**1**]. Among the bio-based polymer matrices being used for the making of bio-nanocomposites, starch, cellulose and PLA are extensively used materials. This is due to numerous advantages such as low cost, abundant availability, biodegradability, biocompatibility, nontoxicity and renewability [**2-4**]. There are additional advantages due to the nano size of the fillers, such as high aspect ratio, high crystallinity, and easy modification to enhance dispersion. Starch nanocrystals can be prepared through acid hydrolysis [**5-7**], enzymatic hydrolysis [**8**], a combined enzymatic and acid hydrolysis [**9**], and high pressure homogenization [**10**]. Starch nanocrystals have been used as reinforcement in various polymers to improve the mechanical strength [**11-15**], and since SNC have platelet like shape they have been used as nanofiller to improve the barrier properties [**16-18**]. To overcome the inherent limitations of PLA which include

brittleness, poor thermal resistance, poor barrier properties and difficulties in achieving mechanical properties as compared to commercial polymers while retaining the biodegradability, PLA based high performance nanocomposites can be prepared using WSNC as nanofiller [**4**].

Although these polymers are claimed to be biodegradable when they move in the waste stream, at present there is no standardized technique to determine exactly how rapidly they disintegrate in the environment. It would be interesting to observe the effects of incorporating nanofillers such as starch nanocrystals on the degradation characteristics of the nanocomposites. Various studies, describing different lab scale methods to evaluate the rate of degradation of biodegradable polymers, are reported in the literature [**19-21**]. Broadly there are two main methods for degradation of polymers, abiotic and biotic. Microbes, as the main source of degradation, are employed in biotic degradation. Further, the two most common forms of biotic degradation with microbes use compost and activated sludge. Abiotic systems use non-microbial methods of degradation such as acid/base hydrolysis [**22**] and photodegradation/ weathering. During acid or base catalyzed hydrolysis, the degradation is initiated by targeting the ether or ester linkage, which is the characteristic functional group of many polymers. The ester bond starts to degrade in the alkaline or acidic atmosphere and the polymer chain is broken to smaller fragments. All the studies mentioned above showed that most of the biotic processes involving microbes take more than four weeks to degrade the polymers. Therefore, there is a need to develop a screening tool or tests, which can be used to measure the relative degradation rate of these polymer composites quickly in lab scale. The results can be useful to compare the rates of degradation of these polymer composites with that of neat biodegradable and non-biodegradable conventional polymers.

In the current study, PLA-WSNC nanocomposites were prepared through melt processing at 170°C, with different concentration of WSNC, to be used for packaging application. The influence of WSNC concentration on the morphological, structural, thermal and degradation properties were investigated.

Experimental

Materials

A commercially available polylactic acid (PLA- 4032D from Nature-Works, molecular weight- 155,000 g/mol, density- 1.24 g/cm^3), high density polyethylene (HDPE), and waxy maize starch (99% amylopectin) were supplied by Sigma-Aldrich. Raw waxy maize starch granules were further hydrolyzed to form WSNC which was used for the preparation of PLA-WSNC nanocomposites.

Synthesis of WSNCs

WSNCs were prepared from acid hydrolysis of waxy maize starch using H_2SO_4 following the optimized procedure described by Angellier *et al.* [**6**]. Waxy maize granules (36.73g) were hydrolyzed in 250 ml of 3.16 M sulfuric acid at 40 °C for five days. After acid hydrolysis, frequent centrifugation of WSNC dispersion was carried out until neutralization was achieved. The solution was then sonicated, in an ultrasonic processor for 30 min surrounded by ice to avoid the heating up of the sample, in order to break the lumps formed during centrifugation and finally freeze-dried at -65 °C to obtain the loose powder of WSNC. WSNC characterization has already been reported in Takkalkar *et al.* [**23**].

Preparation of PLA-WSNC bio-nanocomposites

The PLA-WSNC nanocomposite samples were melt-blended in a Haake Rheomix at 170 ºC for 5 min at 50 rpm at various concentrations of WSNC. PLA and WSNC were dried in a vacuum oven at 80 ºC overnight prior to melt processing to remove any traces of moisture. After mixing, the dried mixture was compression molded at 200 ºC for 5 min with a force of 80 kN to obtain round shaped discs (d 25 mm, t 2 mm). These discs were used for degradation studies.

The PLA-WSNC nanocomposites were prepared by incorporating WSNC in PLA matrix at three different concentrations as shown in **Table 1**. The samples were coded as PLA-WSNC-1 wt%, PLA-WSNC-3 wt% and PLA-WSNC-5 wt% in which the number denoted the concentration (wt%) of WSNC in PLA. Along with this, neat PLA (100%) and neat high density polyethylene (HDPE) (100%) samples were prepared as controls. Neat PLA degradation studies are important in order to understand the type and effect of increasing WSNC content on the nanocomposites. Neat HDPE as a control helps to understand the difference clearly for degradation, as conventional polymers do not degrade.

Table 1. Sample compositions.

	PLA (wt %)	WSNC (wt %)
Neat PLA	100	-
Neat HDPE	100	-
PLA-WSNC-1 wt%	99	1
PLA-WSNC-3 wt%	97	3
PLA-WSNC-5 wt%	95	5

Characterization of PLA-WSNC nanocomposites

Scanning electron microscopy (SEM)

The morphology of the fractured surface of the PLA-WSNC nanocomposites was investigated by means of FEI Quanta 200 ESEM. The samples were dipped in liquid nitrogen and immediately snapped to expose inner morphological features of the films. All the nanocomposites were sputter coated with a thin coat of gold to ensure conduction observed and the images were taken under an accelerating voltage of 10 kV.

Fourier transform infrared spectroscopy (FTIR)

The Fourier transform infrared spectroscopy (FTIR) spectra of the PLA-WSNC nanocomposites were recorded in a PerkinElmer FTIR spectrophotometer.

FTIR spectra were obtained in the wavenumber range from 450 cm^{-1} to 4000 cm^{-1}. 32 scans per sample were accumulated at a resolution of 4 cm^{-1}.

Thermogravimetric analysis (TGA)

Thermogravimetric measurements to examine the thermal stability of the PLA-WSNC nanocomposites were performed in a STA 6000, Perkin-Elmer Instrument, under an instrument air flow of 20 $mLmin^{-1}$. All the PLA-WSNC nanocomposite samples were heated from room temperature to 600°C with a heating rate of 10 °C min^{-1}. Three samples were used to characterize each nanocomposite and sample weight percentage was plotted as a function of temperature.

Modulated differential scanning calorimetry (MDSC)

The effect of incorporating WSNC, at different loadings, on the overall crystallization behavior of the PLA matrix, was studied using modulated differential scanning calorimetry. MDSC analysis of PLA-WSNC nanocomposites was conducted on a DSC-2920 Modulated DSC (TA Instruments), with successive heating, cooling and heating scans. The instrument calibration was performed with indium in a nitrogen environment; with a 35 ml/min flow rate. Unfilled aluminum pan sealed with a lid was taken as a reference. PLA-WSNC nanocomposites samples with weight approximately 7-10 mg were encapsulated in aluminum pans. All the nanocomposites were scanned over a range of -20 °C to 220 °C at a 2 °C/min heating rate and modulated +/- 0.50 °C every 40 seconds. Prior to this scan, a pretreatment heating and cooling scan was employed to erase the thermal history. Glass transition, cold crystallization and melting temperatures and the respective enthalpies were obtained from the second heating scan.

Dilute alkali-catalysed hydrolysis

1M Sodium hydroxide solution was used for the hydrolysis study of the PLA-WSNC nanocomposites which was prepared with de-ionized water. Three specimens from each nanocomposite sample disc were weighed on a Denver analytical balance to five decimal places prior to placing them in a glass beaker and immersed in NaOH solution. Neat HDPE sample disc was placed in NaOH solution as negative control. The beakers with NaOH solution and PLA-WSNC nanocomposites samples were then covered with aluminum foil and stored at 25°C and 50-60% relative humidity. Each specimen disc was weighed by initially taking out the discs from alkaline solution with forceps, absorbing the excess solution from the surface of discs with paper towels, to get accurate weights. After weighing all the samples were placed in the respective beakers, covered and stored. Using the initial weight of the nanocomposites, the percentage weight loss was calculated and plotted vs. time.

Results and discussion

Morphology of PLA-WSNC nanocomposites

The distribution level of WSNC inside the PLA matrix was evaluated by observing the SEM image of the cryo-fractured surface of the PLA-WSNC nanocomposites (**Fig. 1**). It can be seen from **Fig. 1(a)** that the neat PLA being amorphous polymer has a smooth and brittle surface than that of the PLA-WSNC nanocomposites [**24, 25**]. Smooth morphology for neat PLA has been reported previously by Mukherjee *et al.* [**26**]. A homogeneous distribution of WSNC can be seen in the PLA-WSNC nanocomposites with the lower concentration of WSNC (**Fig. 1(b)** and **Fig. 1(c)**). Uniform distribution of the nanofiller within the polymer matrix is reported as important for attaining optimum properties [**27**]. At the highest loading of WSNC (5 wt%) there was a tendency to agglomerate (circles) which can be clearly observed in **Fig. 1(d)**, overall which results in a rougher surface. The surfaces of the PLA-WSNC nanocomposites also showed the formation of small voids or indications of crystals pull-out (arrows) [**28**]. The formation of agglomerates at higher loadings was apparently due to the presence of strong hydrogen bonding within the WSNC [**29**].

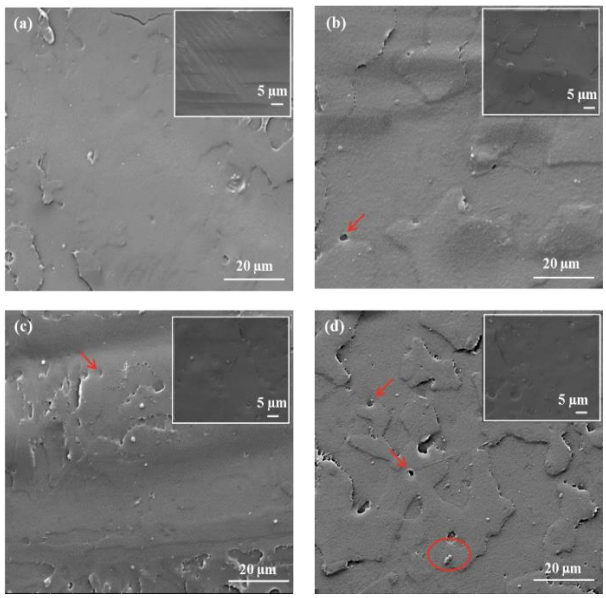

Fig. 1. SEM images of (a) PLA, (b) PLA-WSNC-1 wt %, (c) PLA-WSNC-3 wt %, (d) PLA-WSNC-5 wt %.

FT-IR nanocomposites

The FT-IR analysis has been broadly used to investigate the interfacial behavior of polymer nanocomposites [**30, 31**]. The characteristic FT-IR spectra, within the 4000-500 cm^{-1} region, of neat PLA and PLA-WSNC nanocomposites are shown in **Fig. 2**. The band originating from C=O stretching vibration of ester carbonyl is located at 1750 cm^{-1}. This is in accordance with the literature [**32-34**]. The peaks corresponding to the distortion of C-H in CH_3 appeared at 1450 cm^{-1} [**31**]. The peak at 871 cm^{-1} is accredited to C-C single bond

stretching vibration. The peak at 1181, 1130, and 1080 cm^{-1} correspond to the stretching of C-O bond [**30**]. As observed from the spectra of the nanocomposites, there is no new peak formation after the addition of low concentrations of WSNC. This is an indication that there is more of physical interaction between the nanofiller and the matrix and no noteworthy chemical interaction. Similar outcomes have been described previously for PLA and cellulose based composites and nano-composites [**31, 35**]. However, with the increase in concentration of WSNC, the peak at 1750 cm^{-1} for C=O stretching became slightly broader. This can be accredited to the interfacial interaction between the O-H group of WSNC and C=O of PLA [**30**]. FT-IR spectra revealed the miscibility and improved the molecular interaction between PLA and WSNC.

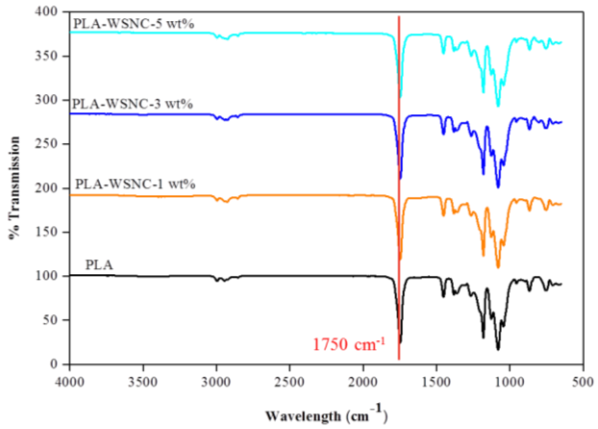

Fig. 2. FTIR spectra of PLA-WSNC nanocomposites with 0-5 wt% of WSNC.

Thermal degradation behaviour of PLA-WSNC nanocomposites

The TG and DTG curves are presented in **Fig. 3(a)** and **Fig. 3(b)**, respectively, which shows weight (%) and derivative (%/min) vs. sample temperature of PLA-WSNC nanocomposites. The thermal stability of nanocomposite is an important aspect which can influence the potential use of WSNC as reinforcement in PLA matrix. The temperatures at which the 5%, 10% and 50% weight loss (WL) of the material occurred and other key thermal factors attained from TG and DTG are presented in **Table 2**. All the PLA-WSNC nano-composites degraded in a single stage as expected. The addition of WSNC moved the onset of degradation to lower temperatures than that of neat PLA. This indicated a slight reduction in thermal stability of the PLA-WSNC nanocomposites. This can be attributed to the fact that WSNC have inherently lower thermal stability as they have hydroxyl groups on their surface which can be hydrogen bonded to PLA [**24, 23, 36**]. In addition, the WSNC were prepared using an acid hydrolysis treatment (sulfuric acid) and the WSNC may contain some sulfate groups which catalyze this degradation process [**37**]. However, as observed from T_{max} there was no degradation taking place in the temperature region, where the PLA-WSNC nanocomposites are intended to be processed (25-200 ºC) [**38,39**]. The T_{max} for PLA and PLA-WSNC nanocomposites (at WSNC conc of 1, 3 and 5 wt%) are 357 ºC, 355 ºC, 350 ºC and 351 ºC, respectively. The T_{max} for melt processed PLA is in agreement with the literature [**37**]. Usually above 300 ºC, neat PLA shows substantial thermal degradation due to lactide reformation, hydrolysis, intramolecular trans-esterification and oxidative chain scission effect [**40**].

It is interesting to note that PLA-WSNC-3 wt% displayed highest amount of char residue in comparison to neat PLA, PLA-WSNC-1 wt% and PLA-WSNC-5 wt%. This trend could be possibly due to the presence of higher loadings of WSNC which has been reported to possess flame resistant property owing to the presence of sulfate groups on them [**36**]. According to Hapuarachchi, Peijs [**41**], a material leaving a higher char residue is important in terms of providing an effective barrier for volatile gases by creating a tortuous path.

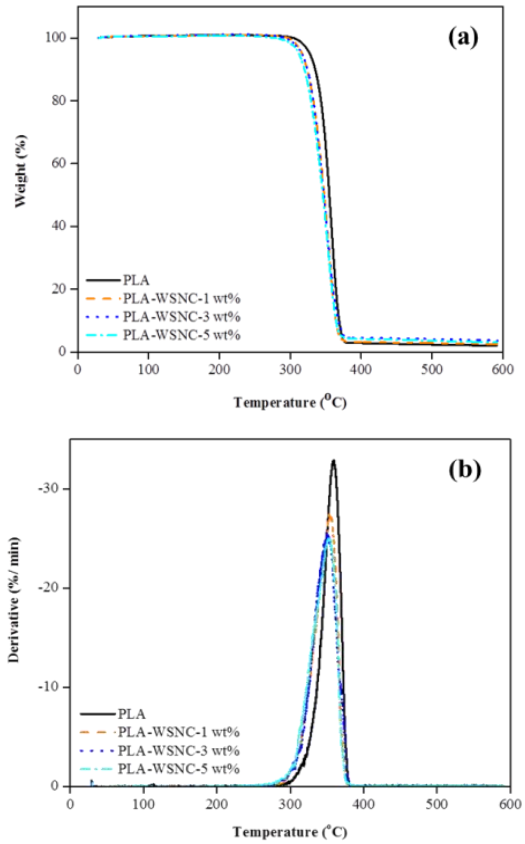

Fig. 3. (a) TGA and (b) DTG curves of PLA-WSNC nanocomposites with 0-5 wt% of WSNC.

Table 2. TGA data of PLA-WSNC nanocomposites.

Sample	$T_{5\%WL}$	$T_{10\%WL}$	$T_{50\%WL}$	Wt % left at 500 °C	T_{max}
PLA	327± 2.05	334± 1.56	353± 0.59	2.1± 0.46	357± 1.25
PLA-WSNC-1 wt%	318± 2.28	325± 1.07	348± 0.07	2.6± 0.58	355± 1.08
PLA-WSNC-3 wt%	312± 1.27	320± 2.08	345± 1.29	3.4± 0.97	350± 0.13
PLA-WSNC-5 wt%	311± 1.92	319± 1.76	345± 2.06	3.3± 0.69	351± 0.69

MDSC nanocomposites

MDSC helps to understand the interactions between the nanofiller and PLA matrix and the crystalline properties of the nanocomposites by observing the variations in the glass transition and cold crystallization temperature [**33**]. MDSC thermograms of PLA-WSNC nanocomposites are shown in **Fig. 4 (a)**. The values for the glass transition temperature (T_g), change in reverse heat capacity (ΔC_p), cold crystallization temperature (T_{cc}), exothermic enthalpy of crystallization (ΔH_{cc}), melting point (T_m), endothermic enthalpy of melting (ΔH_m), and the degree of crystallinity (X_c) of the PLA-WSNC nanocomposites are summarized in **Table 3**. The data from **Table 3** for T_g, showed that there was no obvious change in T_g for the PLA-WSNC nanocomposites; this is in accordance with the previous published research [**24, 32**]. The endothermic peak corresponding to melting temperatures did not vary significantly with respect to neat PLA, which is around 168 ºC. The T_m depends largely on the dimensions and perfection of the crystal-like structures, no deviation in this indicated that the crystalline lamellae of nanocomposites after the recrystallization process were not changed [**42, 43**]. The effect of incorporating WSNC on the nucleation of crystals within the nanocomposites could be interpreted through the change in T_{cc}. The T_{cc} of neat PLA was highest and it continued to drop with the increase in loading of WSNC, this is an indication of faster crystallization [**43**]. Similar trend for PLA based nanocomposites with cellulose and chitin nanocrystals as nanofiller has been reported in the literature [**26, 44, 45**]. The reduction in T_{cc} is attributed to the enhancement in the rate of nucleation and promoting crystallization within the nanocomposites [**46-48**]. The decline in the T_{cc} and increase in crystallinity for PLA-WSNC nanocomposites indicated that the WSNC act as nucleating agents of PLA matrix and increase the nucleus density of PLA crystallites [**49, 50**]. The addition of WSNC favored PLA recrystallization [**51, 32**]. The crystalline properties of the nanocomposites were elevated at lower loadings due to nucleation function of nanocrystals [**33**]. The percent crystallinity (X_c) of neat PLA and PLA-WSNC nanocomposites was calculated using Eq. (1):

$$Xc = 100 \times \left[\frac{\Delta H_m - \Delta H_{cc}}{\Delta H_m^c}\right] \times \frac{1}{W_{PLA}} \quad (1)$$

where ΔH_m (Jg^{-1}) is the melting enthalpy, ΔH_{cc} (Jg^{-1}) is the cold crystallization enthalpy, ΔH_m^c is the melting enthalpy of pure PLA (93 Jg^{-1}) [**52,53**] and W_{PLA} is the weight fraction of PLA in the PLA-WSNC bio-nanocomposites. The calculated results are listed in **Table 3**. The overall percentage crystallinity is slightly higher for PLA-WSNC-3 wt% than the rest of the nanocomposites, indicating the positive effect of adding WSNC. It is also evident from the SEM that the dispersion is more uniform for PLA-WSNC-3 wt%, the nucleating effect is enhanced and consequently it results in higher crystallinity [**24**]. The nucleation effect is improved when a more homogeneous dispersion is achieved and this ultimately increases the crystallinity of the nanocomposites [**51, 38**]. In the case of PLA-WSNC-5 wt%, the self-agglomerated WSNC induce a reduction in overall crystallinity. These results are in accordance with the morphological results.

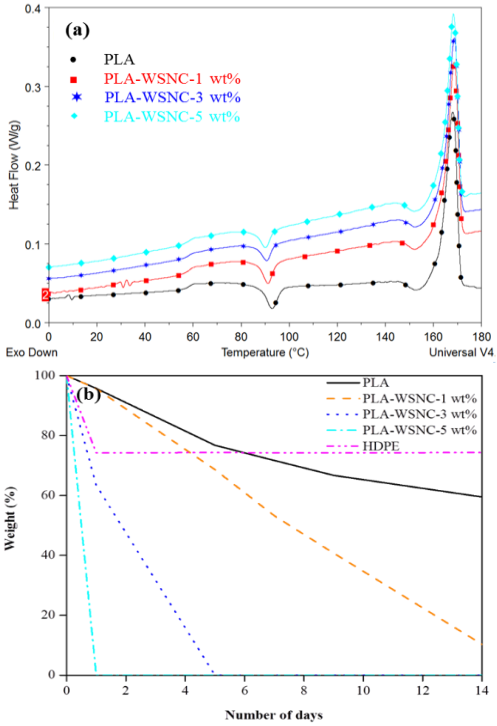

Fig. 4. (a) MDSC thermograms of PLA-WSNC nanocomposites with 0-5 wt% of WSNC from second heating cycle, and (b) Weight % of PLA-WSNC nanocomposites vs. time (days).

Degradation studies of nanocomposites

Although PLA is biodegradable, its slow degradation rate when matched to other polymers is an important issue [**54, 55**]. Hydrolytic degradability of PLA-WSNC nanocomposites was studied by assessing the effect of base catalyst. For each nanocomposite the change in its weight due to hydrolytic degradation was recorded with time (days). The reduction in weight was plotted in terms of weight % vs time as shown in **Fig. 4 (b)**. Degradation

Table 3. MDSC Analysis of Neat PLA and PLA-WSNC nanocomposites from second heating cycle.

Sample	SNC (wt %)	T_g (°C)	ΔC_p J/(g·°C)	T_{cc} (°C)	ΔH_{cc} (Jg^{-1})	T_m (°C)	ΔH_m (Jg^{-1})	X_c(%)
PLA-Neat	0.00	58.8	0.3	93.1	7.0	168.0	41.6	37.2
PLA-WSNC-1 wt%	1.00	58.6	0.2	91.2	5.0	168.4	39.7	37.7
PLA-WSNC-3 wt%	3.00	58.3	0.2	90.4	4.2	168.3	39.0	38.6
PLA-WSNC-5 wt%	5.00	58.9	0.2	90.1	6.2	168.3	39.2	37.4

in alkaline environments was initially assessed by the visual observation of the PLA-WSNC nanocomposites, wherein it was detected that the nanocomposite discs begin to fragmentize from the first day. It can be noted that there is a continuous decrease in weights of all nanocomposites.

Fig. 4 (b) revealed that the negative control HDPE (100%) tends to lose a small amount of weight within one day, but stays fairly constant after that. This confirms that the conventional polymers cannot be broken down easily and they have high resistance towards alkaline hydrolysis. In the early stages of degradation, due to alkaline conditions, the hydrolysis of high molecular weight PLA chains to low molecular weight is initiated [**22**]. The smaller molecules are formed due to the chain scission of long molecules [**56**]. Jung *et al.* [**22**] reported a comparison study of hydrolytic degradation of poly(propylene carbonate) (PPC), poly(e-caprolactone) (PCL) and poly(D,L-lactic acid) (PLA) in acidic and alkaline conditions. The results showed that all evaluated polymers, indicated higher rate of degradation in strong alkaline environments than in strong acidic environments. The faster degradation rate in alkaline conditions was ascribed to high electrophilicity of the carbonyl atoms present in the backbone of the polymer [**22**]. It can be noted that PLA-WSNC-5 wt% and PLA-WSNC-3 wt% were the fastest to diminish, the reason being the highest concentration of WSNC- 5 wt% and 3 wt%, respectively. The complete degradation of PLA-WSNC-5 wt% and PLA-WSNC-3 wt% at day 1 can be possibly due to the occurrence of hydroxyl groups on the surface of WSNC nanofiller that renders a catalytic role to hydrolyze the ester groups in the PLA. The complex process of degradation of PLA can be accelerated by any factor that escalates the hydrolysis process of PLA [**54**]. Samples with lower WSNC content, i.e. PLA-WSNC-1 wt% degraded slowly but completely over a period of 14 days.

Overall the degradation test revealed that PLA-WSNC nanocomposites were evidently disintegrated after 14 days, and HDPE being the conventional non-biodegradable polymer, was obviously present at day 14. Also, the degradation rate is highly reliant on the concentration of WSNC within PLA, the higher the WSNC the faster the degradation. The biodegradation extent when compared to other systems is far more accelerated; this can be ascribed to the nanosize of WSNC nanofiller, which led to complete biodegradation of the samples [**20**]. It can be observed that with this method it is easy to trace the extent of biodegradation of any bio-nanocomposites.

Conclusions

PLA-WSNC based nanocomposites were prepared by melting and mixing in a Haake rheomix at different loadings of WSNC. Morphological analysis showed that the WSNC disperse well at lower loadings (1 wt% and 3 wt%) and tend to agglomerate at higher loadings (5 wt%), in the PLA matrix. FT-IR spectra showed no new peak formation with increase in concentration of WSNC, however there was slight broadening of the carbonyl peak in all the nanocomposites. This indicated a remarkable physical interaction between the nanofiller and the matrix, with no significant chemical interaction. The nanocomposites were safe to be processed in the commercial processing temperature range (25-200 ºC). MDSC study showed that there were no noteworthy changes in the glass transition and melting temperatures, though the cold crystallization temperature was reduced, which suggested enhancement in the nucleation rate and ultimately increased in overall crystallinity of the nanocomposites. Abiotic method proved effective as safe, easy and quick laboratory scale screening tool for determining the biodegradability of PLA based nanocomposites. The study showed that WSNC could accelerate the slow degradation process of PLA. WSNC dispersed well in the PLA matrix at lower concentration (1 and 3 wt%) while some of the properties were affected when the concentration increased further, due to agglomeration. Overall the results showed that WSNC have the potential to improve the properties of PLA based nanocomposites.

Acknowledgements

The work reported in this article was financially supported by RMIT University. The authors gratefully acknowledge the technical support from Mike Allan and Dr. Muthu Pannirselvam of the School of Engineering, and Mr. Philip Francis of the RMIT Microscopy and Microanalysis Facility, at RMIT University.

References

1. Mariano, M.; El Kissi, N.; Dufresne, A., Cellulose nanocrystals and related nanocomposites: Review of some properties and challenges. *J. Polym. Sci., Part B: Polym. Phys.*, **2014,** *52*, 791. **DOI:** 10.1002/polb.23490
2. Auras, R.; Harte, B.; Selke, S., An Overview of Polylactides as Packaging Materials. *Macromol. Biosci.*, **2004,** *4*, 835. **DOI:** 10.1002/mabi.200400043
3. Azeredo, H.M.C.; Rosa, M.F.; Mattoso, L.H.C., Nanocellulose in bio-based food packaging applications. *Ind. Crops Prod.*, 97 (Supplement C), **2017,** 664. **DOI:** 10.1016/j.indcrop.2016.03.013
4. Lagarón, J.M., 17 Polylactic acid (PLA) nanocomposites for food packaging applications. Multifunct. Nanoreinf. Polym. Food Packag., *Woodhead Publishing*, **2011,** 485.
5. Putaux, J. L.; Molina-Boisseau, S.; Momaur, T.; Dufresne, A., Platelet nanocrystals resulting from the disruption of waxy maize starch granules by acid hydrolysis. Biomacromolecules, **2003,** *4*, 1198.
6. Angellier, H.; Choisnard, L.; Molina-Boisseau, S.; Ozil, P.; Dufresne, A., Optimization of the preparation of aqueous suspensions of waxy maize starch nanocrystals using a response surface methodology. *Biomacromolecules;* **2004,** *5*, 1545. **DOI:** 10.1021/bm049914u
7. Le Corre, D.; Bras, J.; Dufresne, A., Evidence of micro- and nanoscaled particles during starch nanocrystals preparation and their isolation. *Biomacromolecules;* **2011,** *12*, 3039. **DOI:**10.1021/bm200673n
8. Sun, Q.; Gong, M.; Li, Y.; Xiong, L., Effect of retrogradation time on preparation and characterization of proso millet starch nanoparticles. *Carbohydr. Polym.*, **2014,** *111*, 133. **DOI:** 10.1016/j.carbpol.2014.03.094
9. Le Corre, D.; Vahanian, E.; Dufresne, A.; Bras, J., Enzymatic pretreatment for preparing starch nanocrystals. *Biomacromolecules*, **2011,** *13*, 132. **DOI:** 10.1021/bm201333k

10. Shi, A. M.; Li, D.; Wang, L. J.; Li, B. Z.; Adhikari, B., Preparation of starch-based nanoparticles through high-pressure homogenization and miniemulsion cross-linking: Influence of various process parameters on particle size and stability. *Carbohydr. Polym.*, **2011,** *83*, 1604.
DOI: 10.1016/j.carbpol.2010.10.011
11. Angellier, H.; Molina-Boisseau, S.; Lebrun, L.; Dufresne, A., Processing and Structural Properties of Waxy Maize Starch Nanocrystals Reinforced Natural Rubber. *Macromolecules*, **2005,** *38*, 3783.
DOI: 10.1021/ma050054z
12. Chang, P. R.; Ai, F.; Chen, Y.; Dufresne, A.; Huang, J., Effects of starch nanocrystal-graft-porycaprolactone on mechanical properties of waterborne polyurethane-based nanocomposites. *J. Appl. Polym. Sci.*, **2008,** *111*, 619.
DOI: 10.1002/app.29060
13. Chen, G.; Wei, M.; Chen, J.; Huang, J.; Dufresne, A.; Chang, P.R., Simultaneous reinforcing and toughening: New nanocomposites of waterborne polyurethane filled with low loading level of starch nanocrystals. *Polymer*, **2008,** *49*, 1860.
DOI: 10.1016/j.polymer.2008.02.020
14. Piyada, K.; Waranyou, S.; Thawien, W., Mechanical, thermal and structural properties of rice starch films reinforced with rice starch nanocrystals. *Int. Food Res. J.*, **2012**, *20*, 439.
15. Bel Haaj, S.; Thielemans, W.; Magnin, A.; Boufi, S., Starch nanocrystals and starch nanoparticles from waxy maize as nanoreinforcement: A comparative study. *Carbohydr. Polym.*, **2016,** *143*, 310.
DOI: 10.1016/j.carbpol.2016.01.061
16. Duan, B.; Sun, P.; Wang, X.; Yang, C., Preparation and properties of starch nanocrystals/carboxymethyl chitosan nanocomposite films. *Starch - Stärke*, **2011**, *63*, 528.
DOI: 10.1002/star.201000136
17. LeCorre, D.; Dufresne, A.; Rueff, M.; Khelifi, B.; Bras, J., All starch nanocomposite coating for barrier material. *J. Appl. Polym. Sci.*, **2014,** *131*.
DOI: 10.1002/app.39826
18. Condes, M.C.; Anon, M.C.; Mauri, A.N.; Dufresne, A., Amaranth protein films reinforced with maize starch nanocrystals. *Food Hydrocolloids*, **2015,** *47*, 146.
DOI: 10.1016/j.foodhyd.2015.01.026
19. Jiang, F.; Zhou, X.; Xu, Y.; Zhu, J.; Yu, S., Degradation Profiles of Non-lignin Constituents of Corn Stover from Dilute Sulfuric Acid Pretreatment. *J. Wood Chem. Technol.*, **2015,** *36*, 192.
DOI: 10.1080/02773813.2015.1112403
20. Petinakis, E.; Liu, X.; Yu, L.; Way, C.; Sangwan, P.; Dean, K.; Bateman, S.; Edward, G., Biodegradation and thermal decomposition of poly(lactic acid)-based materials reinforced by hydrophilic fillers. *Polym. Degrad. Stab.*, **2010,** *95*, 1704.
DOI: 10.1016/j.polymdegradstab.2010.05.027
21. Ghanbarzadeh, B.; Almasi, H., Biodegradable Polymers. *Biodegrad.: Life Sci.*, **2013**.
22. Jung, J.H.; Ree, M.; Kim, H., Acid- and base-catalyzed hydrolyses of aliphatic polycarbonates and polyesters. *Catal. Today.*, **2006,** *115*, 283.
DOI: 10.1016/j.cattod.2006.02.060
23. Takkalkar, P.; Ganapathi, M.; Dekiwadia, C.; Nizamuddin, S.; Griffin, G.; Kao, N., Preparation of Square-Shaped Starch Nanocrystals/Polylactic Acid Based Bio-nanocomposites: Morphological, Structural, Thermal and Rheological Properties. *Waste Biomass Valorization.*, **2018**.
DOI: 10.1007/s12649-018-0372-0
24. Fortunati, E.; Luzi, F.; Puglia, D.; Petrucci, R.; Kenny, J.M.; Torre, L., Processing of PLA nanocomposites with cellulose nanocrystals extracted from Posidonia oceanica waste: Innovative reuse of coastal plant. *Ind. Crops Prod.*, **2015**, *67*, 439.
DOI: 10.1016/j.indcrop.2015.01.075
25. Jonoobi, M.; Mathew, A.P.; Abdi, M.M.; Makinejad, M.D.; Oksman, K., A Comparison of Modified and Unmodified Cellulose Nanofiber Reinforced Polylactic Acid (PLA) Prepared by Twin Screw Extrusion. *J. Polym. Environ.*, **2012**, *20*, 991.
DOI: 10.1007/s10924-012-0503-9
26. Mukherjee, T.; Sani, M.; Kao, N.; Gupta, R.K.; Quazi, N.; Bhattacharya, S., Improved dispersion of cellulose microcrystals in polylactic acid (PLA) based composites applying surface acetylation. *Chem. Eng. Sci.*, **2013,** *101*, 655.
DOI: 10.1016/j.ces.2013.07.032
27. Rajisha, K.R.; Maria, H.J.; Pothan, L.A.; Ahmad, Z.; Thomas, S., Preparation and characterization of potato starch nanocrystal reinforced natural rubber nanocomposites. Int. *J. Biol. Macromol.*, **2014,** *67*, 147.
DOI: 10.1016/j.ijbiomac.2014.03.013
28. Herrera, N.; Salaberria, A.M.; Mathew, A.P.; Oksman, K., Plasticized polylactic acid nanocomposite films with cellulose and chitin nanocrystals prepared using extrusion and compression molding with two cooling rates: Effects on mechanical, thermal and optical properties. *Composites Part A.*, **2016**, *83*, 89.
DOI: 10.1016/j.compositesa.2015.05.024
29. Le Corre, D.; Bras, J.; Dufresne, A., Starch nanoparticles: A review. *Biomacromolecules*, **2010,** *11*, 1139.
DOI: 10.1021/bm901428y
30. Qu, P.; Gao, Y.; Wu, G.; Zhang, L., Nanocomposites of poly (lactic acid) reinforced with cellulose nanofibrils. *BioResources*, **2010,** *5*, 1811.
31. Haafiz, M.K.M.; Hassan, A.; Zakaria, Z.; Inuwa, I.M.; Islam, M.S.; Jawaid, M., Properties of polylactic acid composites reinforced with oil palm biomass microcrystalline cellulose. *Carbohydr. Polym.*, **2013**, *98*, 139.
DOI: 10.1016/j.carbpol.2013.05.069
32. Arrieta, M.P.; Fortunati, E.; Dominici, F.; Rayon, E.; Lopez, J.; Kenny, J.M., Multifunctional PLA-PHB/cellulose nanocrystal films: processing, structural and thermal properties. *Carbohydr. Polym.*, **2014**, *107*, 16.
DOI: 10.1016/j.carbpol.2014.02.044
33. Lin, N.; Huang, J.; Chang, P.R.; Feng, J.; Yu, J., Surface acetylation of cellulose nanocrystal and its reinforcing function in poly(lactic acid). *Carbohydr. Polym.*, **2011,** *83*, 1834.
DOI: 10.1016/j.carbpol.2010.10.047
34. Fortunati, E.; Armentano, I.; Iannoni, A.; Barbale, M.; Zaccheo, S.; Scavone, M.; Visai, L.; Kenny, J.M., New multifunctional poly(lactide acid) composites: Mechanical, antibacterial, and degradation properties. *J. Appl. Polym. Sci.*, **2012**, *124*, 87.
DOI: 10.1002/app.35039
35. Yin, Z.; Zeng, J.; Wang, C.; Pan, Z., Preparation and Properties of Cross-Linked Starch Nanocrystals/Polylactic Acid Nanocomposites. *Int. J. Polym. Sci.*, **2015**.
DOI: 10.1155/2015/454708
36. LeCorre, D.; Bras, J.; Dufresne, A., Influence of native starch's properties on starch nanocrystals thermal properties. *Carbohydr. Polym.*, **2012,** *87*, 658.
DOI: 10.1016/j.carbpol.2011.08.042
37. Garcia, N.L.; Lamanna, M.; D'Accorso, N.; Dufresne, A.; Aranguren, M.; Goyanes, S., Biodegradable materials from grafting of modified PLA onto starch nanocrystals. *Polym. Degrad. Stab.*, **2012**, *97*, 2021.
DOI: 10.1016/j.polymdegradstab.2012.03.032
38. Arrieta, M.P.; Fortunati, E.; Dominici, F.; López, J.; Kenny, J.M., Bionanocomposite films based on plasticized PLA–PHB/cellulose nanocrystal blends. *Carbohydr. Polym.*, **2015**, *121*, 265.
DOI: 10.1016/j.carbpol.2014.12.056
39. Petersson, L.; Kvien, I.; Oksman, K., Structure and thermal properties of poly(lactic acid)/cellulose whiskers nanocomposite materials. *Compos. Sci. Technol.*, **2007**, *67*, 2535.
DOI: 10.1016/j.compscitech.2006.12.012
40. Kopinke, F.D.; Remmler, M.; Mackenzie, K.; Möder, M.; Wachsen, O., Thermal decomposition of biodegradable polyesters-II. Poly (lactic acid). *Polym. Degrad. Stab.*, **1996**, *53*, 329.
41. Hapuarachchi, T.D.; Peijs, T., Multiwalled carbon nanotubes and sepiolite nanoclays as flame retardants for polylactide and its natural fibre reinforced composites. *Composites Part A.*, **2010**, *41*, 954.
42. Liu, Y.; Donovan, J.A., Miscibility and crystallization of semicrystalline nylon 6 and amorphous nylon 6IcoT blends. *Polymer*, **1995**, *36*, 4797.

43. Frone, A.N.; Berlioz, S.; Chailan, J.F.; Panaitescu, D.M., Morphology and thermal properties of PLA–cellulose nanofibers composites. *Carbohydr. Polym.,* **2013,** *91*, 377. **DOI:** 10.1016/j.carbpol.2012.08.054
44. Singh, A.A.; Geng, S.; Herrera, N.; Oksman, K., Aligned plasticized polylactic acid cellulose nanocomposite tapes: Effect of drawing conditions. *Composites Part A.*, **2018**, *104,* 101. **DOI:** 10.1016/j.compositesa.2017.10.019
45. Singh, A.A.; Wei, J.; Herrera, N.; Geng, S.; Oksman, K., Synergistic effect of chitin nanocrystals and orientations induced by solid-state drawing on PLA-based nanocomposite tapes. *Compos. Sci. Technol.,* **2018**, *162*, 140. **DOI:** 10.1016/j.compscitech.2018.04.034
46. Reinsch, V.E.; Kelley, S.S., Crystallization of poly (hydroxybutrate-co-hydroxyvalerate) in wood fiber-reinforced composites. *J. Appl. Polym. Sci.,* **1997**, *64*, 1785. **DOI:** 10.1002/(SICI)1097-4628(19970531)64:9<1785::AID-APP15>3.0.CO;2-X
47. Harris, A.M.; Lee, E.C., Improving mechanical performance of injection molded PLA by controlling crystallinity. *J. Appl. Polym. Sci.,* **2008**, *107*, 2246. **DOI:** 10.1002/app.27261
48. Sullivan, E.; Moon, R.; Kalaitzidou, K., Processing and Characterization of Cellulose Nanocrystals/Polylactic Acid Nanocomposite Films. *Materials,* **2015**, *8,* 8106. **DOI:** 10.3390/ma8125447
49. Raquez, J.M.; Murena, Y.; Goffin, A.L.; Habibi, Y.; Ruelle, B.; DeBuyl, F.; Dubois, P., Surface-modification of cellulose nanowhiskers and their use as nanoreinforcers into polylactide: A sustainably-integrated approach. *Compos. Sci. Technol.,* **2012**, *72*, 544. **DOI:** 10.1016/j.compscitech.2011.11.017
50. Li, H.; Cao, Z.; Wu, D.; Tao, G.; Zhong, W.; Zhu, H.; Qiu, P.; Liu, C., Crystallisation, mechanical properties and rheological behaviour of PLA composites reinforced by surface modified microcrystalline cellulose. *Plast., Rubber Compos.,* **2016**, *45*, 181. **DOI:** 10.1179/1743289815Y.0000000040
51. Fortunati, E.; Armentano, I.; Zhou, Q.; Iannoni, A.; Saino, E.; Visai, L.; Berglund, L.A.; Kenny, J.M., Multifunctional bionanocomposite films of poly(lactic acid), cellulose nanocrystals and silver nanoparticles. *Carbohydr. Polym.,* **2012**, *87*, 1596. **DOI:** 10.1016/j.carbpol.2011.09.066
52. Turner, J.; Riga, A.; O'Connor, A.; Zhang, J.; Collis, J., Characterization of drawn and undrawn poly-L-lactide films by differential scanning calorimetry. *J. Therm. Anal. Calorim.,* **2004**, *75*, 257.
53. Mathew, A.P.; Oksman, K.; Sain, M., The effect of morphology and chemical characteristics of cellulose reinforcements on the crystallinity of polylactic acid. *J. Appl. Polym. Sci.,* **2006**, *101*, 300. **DOI:** 10.1002/app.23346
54. Ray, S.S.; Okamoto, M., Biodegradable polylactide and its nanocomposites: opening a new dimension for plastics and composites. Macromol. *Rapid Commun.,* **2003**, *24,* 815.
55. Ozkoc, G.; Kemaloglu, S., Morphology, biodegradability, mechanical, and thermal properties of nanocomposite films based on PLA and plasticized PLA. *J. Appl. Polym. Sci.,* **2009**, *114*, 2481. **DOI:** 10.1002/app.30772
56. Araujo, A.; Oliveira, M.; Oliveira, R.; Botelho, G.; Machado, A.V., Biodegradation assessment of PLA and its nanocomposites. Environ. *Sci. Pollut. Res.,* **2014**, *21*, 9477. **DOI:** 10.1007/s11356-013-2256-y

